



Full Length Article

Ground state parameters, electronic properties and elastic constants of CaMg₃: DFT study

H. Rekab-Djabri^{a,b}, Manal M. Abdus Salam^{c,*}, S. Daoud^d, M. Drief^e, Y. Guermit^e,
S. Louhibi-Fasla^a

^aLaboratory of Micro and Nanophysics (LaMiN), National Polytechnic School Oran, ENPO-MA, BP 1523, El M'Naouer, 31000 Oran, Algeria

^bFaculty of Nature and Life Sciences and Earth Sciences, Akli Mohand-Oulhadj University, 10000 Bouira, Algeria

^cDepartment of Applied Physics, Tafila Technical University, Tafila 66110, Jordan

^dLaboratory of Materials and Electronic Systems, Mohamed El Bachir El Ibrahimi University of Bordj Bou Arreridj, Bordj BouArreridj 34000, Algeria

^eLaboratoire des Matériaux Magnétiques, Département de Physique, Université Djilali LIABES de Sidi-Bel-Abbès, Sidi Bel Abbès 22000, Algeria

Received 24 February 2020; received in revised form 4 June 2020; accepted 17 June 2020

Available online xxx

Abstract

The present study aims to investigate the equation of state (EOS) parameters of CaMg₃ in α ReO₃ (D0₉), AlFe₃ (D0₃), Cu₃Au (L1₂) and CuTi₃ (L6₀) structures, using full potential linear muffin-tin orbitals (FP-LMTO) approach based on the density functional theory (DFT). The local density approximation (LDA) and the generalized gradient approximation (GGA) were both applied for the exchange-correlation potential term. The calculated equation of state parameters at equilibrium, in general, agreed well with the available data of the literature. The calculations showed that under compression CaMg₃ transforms from D0₃ to D0₉ at about 29.96 GPa, and 25.1 GPa using LDA and GGA, respectively.

The elastic constants C_{ij} , aggregate moduli, Vickers hardness, sound velocity, and Debye temperature of CaMg₃ in D0₃ structure were also reported, discussed and analyzed. Using LDA (GGA), the calculated values of H_V and θ_D were found at around 5.80 GPa (5.93 GPa) and 393.44 K (389.91 K), respectively.

Electronic band structure, total density of states (TDOS) as well as the partial density of states (PDOS) have been also obtained. The electronic band structure confirms the metallic behavior of CaMg₃ in D0₃ phase, the valence bands are dominated by the maximum contribution of 'd' like states of Ca in the energy ranging from 2 to 3 eV for GGA, and from 4.5 to 5 eV for LDA, respectively.

© 2020 Published by Elsevier B.V. on behalf of Chongqing University.

This is an open access article under the CC BY-NC-ND license (<http://creativecommons.org/licenses/by-nc-nd/4.0/>)

Peer review under responsibility of Chongqing University

Keywords: CaMg₃ compound; Electronic properties; Phase transition; Elastic constants; FP-LMTO.

1. Introduction

Magnesium (Mg) is an abundant element in the world compared with other commonly used metals; it is one of the lightest among several commonly used structural metals. One of its major advantages is the low density, it is about one quarter that of steels and two thirds that of aluminum [1]. Furthermore, Mg-based alloys, like the binary systems of Mg–Cu

and Mg–Ca, have gained more attention in the last decade. These materials have several applications in engineering, especially in aerospace manufacturing field and automotive industry [2–6]. The binary system of Mg–Ca is potentially used as biomaterial and has been a subject of research by many investigators in recent years [7],[8].

Zhou and Gong [8] have studied the electronic properties, mechanical moduli, chemical bonding and many other parameters of Mg–Ca system in different configurations. Their calculations showed that both BCC (AlFe₃-type structure (D0₃)) and FCC (Cu₃Au-type structure (L1₂)) phases of CaMg₃

* Corresponding author.

E-mail address: manalab70@yahoo.com (M.M.A. Salam).

<https://doi.org/10.1016/j.jma.2020.06.007>

2213-9567/© 2020 Published by Elsevier B.V. on behalf of Chongqing University. This is an open access article under the CC BY-NC-ND license (<http://creativecommons.org/licenses/by-nc-nd/4.0/>) Peer review under responsibility of Chongqing University

Table 1

Plane wave number NPLW, muffin-tin radius (RMT) (in a.u.) and the energy cut-off (in Ry) used in our calculation.

Parameters		αReO_3 (D ₀)	AlFe ₃ (D ₀)	Cu ₃ Au (L ₁)	CuTi ₃ (L ₆)
Total NPLW	LDA	6120	5002	5421	7454
	GGA	11,042	11,212	12,546	14,838
RMTS (Ca)	LDA	2.62	3.21	3.17	3.224
	GGA	2.63	3.15	3.284	3.224
RMTS (Mg)	LDA	2.71	2.75	3.07	3.103
	GGA	2.82	2.70	3.098	3.103
E_{cut}	LDA	12.02	11.5	14.5	71
	GGA	14.1	12.1	14.8	75
K-Point	LDA	(44, 44, 44)	(46, 46, 46)	(38, 38, 38)	(44, 44, 49)
	GGA	(40, 40, 40)	(40, 40, 40)	(42, 42, 42)	(44, 44, 49)

are mechanically stable at equilibrium. Also, they investigated phase transition and found that both AlFe₃-type structure (D₀) and Cu₃Au-type structure (L₁) transform to the hexagonal close packed HCP-type structure (A3) at pressures around 29.47 GPa and 26.44 GPa, respectively. Actually, it is known that under the effect of hydrostatic compression, the crystal often transforms from the most energetic stable phase to another crystallographic configuration [9],[10].

Groh [11] has investigated several physical, mechanical, and thermal properties of pure Calcium (Ca) and Mg–Ca binary system, in the framework of the second nearest-neighbors modified embedded-atom method (MEAM). His results showed also that both AlFe₃-type structure (D₀) and Cu₃Au-type structure (L₁) of CaMg₃ are mechanically stable at equilibrium.

Furthermore, to the best of our knowledge, the CaMg₃ phases of Mg–Ca binary system is not synthesized until now, and it is very difficult to obtain the physical properties of all phases by using the experimental measurement. Under this situation, the first-principles calculations can be applied to compute various physical properties of different phases based on the crystal structural information. In order to further improve the properties of Mg–Ca alloys, a systematic investigation and accurate information on the mechanical properties of some other structures in binary Mg–Ca system is the prerequisite. In the present study, we investigate the equation of state (EOS) parameters, pressure-induced phase transition, elastic constants and electronic properties of CaMg₃ compound using first-principles total energy calculations in the framework of density functional theory (DFT), within both the local density approximation (LDA) [12] and the generalized gradient approximation (GGA) [13].

In Section 2 we introduce a brief description of the method used in this work. Then, we present, in Section 3 our obtained results of the structural parameters, high-pressure induced phase transitions, elastic constants as well as the electronic properties of CaMg₃ compound. Finally, a brief conclusion is given in Section 4.

2. Computational details

The chemical and physical properties of system are determined by the inter-atomic interactions, which can be described by the inter-atomic interaction potential. The calcu-

lations in the present work were made using the all-electron full potential linear muffin-tin orbital (FP-LMTO) augmented by a plane-wave basis (PLW) [14] within the framework of density functional theory (DFT). Unlike the previous LMTO methods, the present version treats both the interstitial regions and the core regions on the same footing [14]. The exchange correlation energy of electrons is described using both the local density approximation (LDA) [12] and the generalized gradient approximation (GGA) as parameterized by Perdew et al. [13].

In FP-LMTO approach, the non-overlapping muffin tin spheres MTS potential is expanded in terms of spherical harmonics inside the spheres of radius RMTS, while in the interstitial region, the s, p and d basis functions are expanded in a number (NPLW) of plane waves determined automatically by the cut-off energies. The details of calculations are as follows: the charge density and the potential are represented inside the muffin-tin (MT) spheres by spherical harmonics up to $l_{max}=6$. The self-consistent calculations are considered to be converged when total energy of the system is stable within 10^{-4} Ry, while self consistent convergence of forces was achieved to within 2×10^{-3} Ry/bohr in ionic minimization. A total energy convergence tests are performed by varying both: plane waves' number PW and cut-off energy E_{cut} . The number of plane waves (NPLW), total cut-off energies, and the muffin-tin radius (RMT) values used in our calculation for our material of interest are summarized in Table 1.

The structures with cubic symmetry (αReO_3 -type (D₀), AlFe₃-type (D₀), which is described as cubic close packed (CCP) cell and Cu₃Au-type (L₁) which is described as an ordered CCP cell), have only one structural parameter (the lattice constant a) that is used to describe the unit cell, while the CuTi₃-type (L₆) having tetragonal symmetry, two structural parameters (a and c/a ratio) are used to describe the unit cell.

The locations of atoms for each crystallographic configuration are also presented in Fig. 1, while the positions of different atoms, as well as the space group for each of the considered structures of CaMg₃ are summarized in Table 2. From Fig. 1, we can observe that the unit cell contains four molecules of CaMg₃ in D₀ structure, while in all other phases (D₀, L₁ and L₆) only one molecule was observed.

Table 2

Location of different atoms and space group of each type of structure of CaMg_3 compound. Pm-3m : Cubic Primitive (cP), Fm-3m : Face-centered cubic (FCC), P4/mmm: Tetragonal Primitive (tP).

	Ca Mg				Space Group
	1st atom	1st atom	2nd atom	3rd atom	
αReO_3 ($D0_9$)	0.0; 0.0; 0.0	0.0; 0.0; 1/2	1/2 ; 0.0; 0.0	0.0; 1/2; 0.0	Pm-3m
AlFe_3 ($D0_3$)	0.0; 0.0; 0.0	1/2; 0.0; 0.0	-1/4; -1/4; -1/4	1/4; 1/4; 1/4	Fm-3m
Cu_3Au ($L1_2$)	0.0; 0.0; 0.0	0.0; 1/2; 1/2	1/2; 0.0; 1/2	1/2; 1/2; 0.0	Pm-3m
CuTi_3 ($L6_0$)	0.0; 0.0; 0.0	1/2; 1/2; 0.0	0.0; 1/2; 1/2	1/2; 0.0; 1/2	P4/mmm

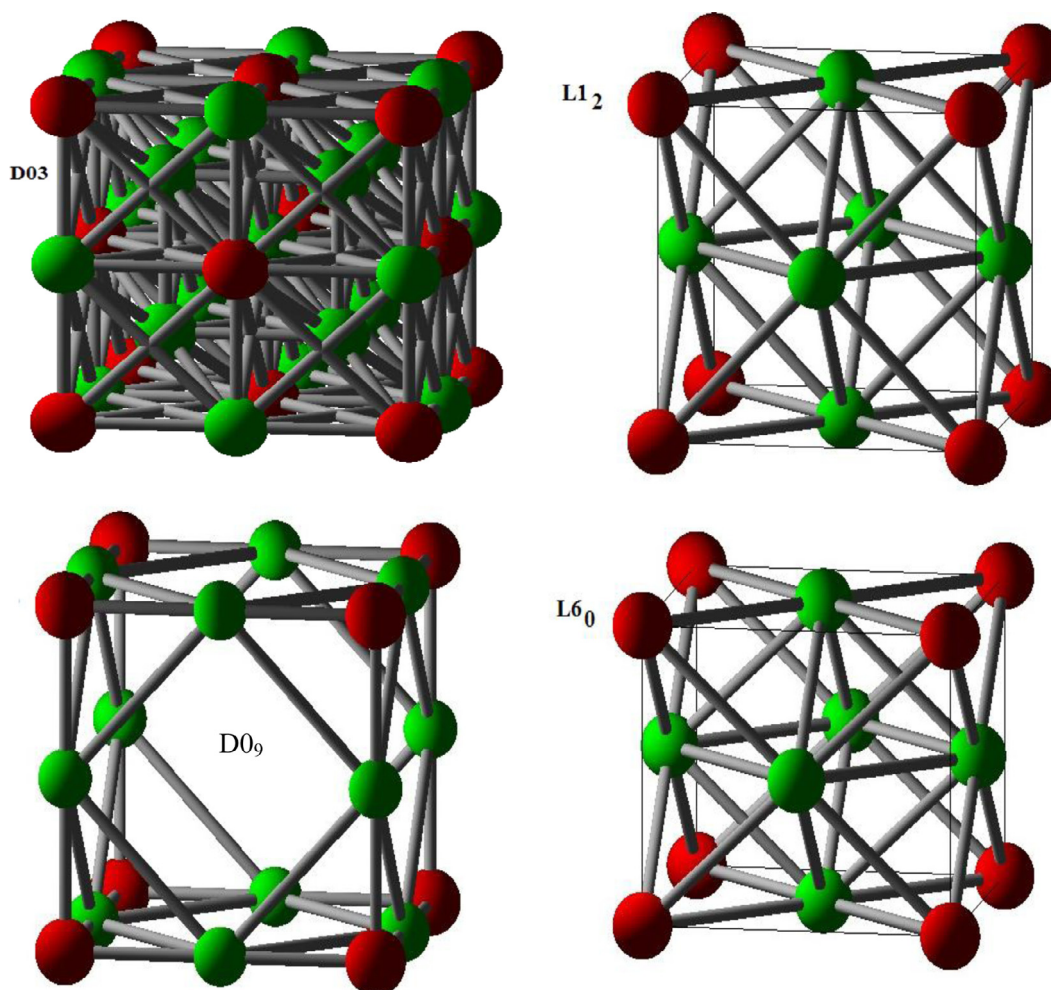


Fig. 1. Cubic and tetragonal crystal structures of CaMg_3 : Ca atoms in red, and Mg atoms in green.

From Fig. 1, we can observe that in $D0_3$ structure, the Ca atoms occupy the positions of the CCP structure and the Mg atoms fill all of the octahedral voids; while in $L1_2$ structure the Ca atoms occupy the cell vertices, while the Mg atoms occupy the face centers. The $L1_2$ structure is just that of cubic Perovskite (CaTiO_3 ($E2_1$)) without the Titanium atoms, and replacing the atoms of Oxygen O per those of Magnesium Mg.

The $L6_0$ structure ($a=b \neq c$) is a tetragonal distortion of $L1_2$ structure ($a=b=c$), so when $c=a$, the atoms are at the positions of a face centered cubic lattice, and with consequence $L6_0$ structure becomes that of $L1_2$.

3. Results and discussion

3.1. Equation of state parameters

In order to investigate the ground state parameters, the total energy at different volumes (E-V) around the equilibrium one is usually determined [15]–[17], and this is how we obtained the structural parameters of different phases of CaMg_3 compound in the present work. These parameters can be also predicted from *ab-initio* calculation of the pressure versus unit cell volume (P-V) data [18]. The equilibrium lattice volume V_0 , bulk modulus B_0 and the pressure derivative

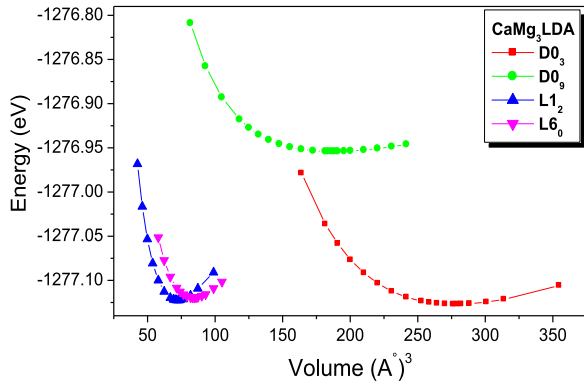


Fig. 2. Total energy versus volume for different structures of CaMg_3 compound using LDA.

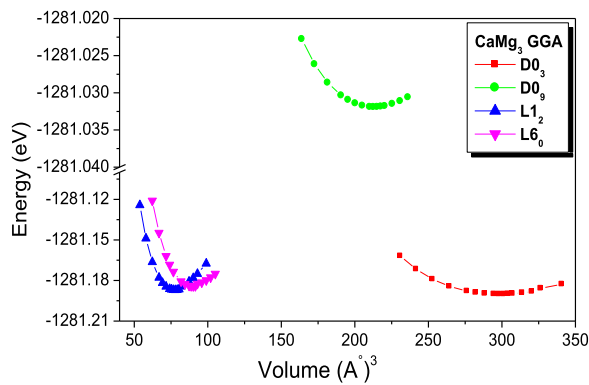


Fig. 3. Total energy versus volume for different phases of CaMg_3 compound using GGA.

of the bulk modulus B_0' have been computed by minimizing the total energy by means of Murnaghan's equation of state (EOS), which can be expressed as [15]:

$$E(V) = E(V_0) + \frac{B_0 V}{B_0'} \left[\frac{(V_0/V)^{B_0'} + 1}{B_0' - 1} \right] - \frac{B_0 V_0}{B_0' - 1} \quad (1)$$

In Eq. (1), E_0 is the energy of the ground state, corresponding to the equilibrium volume V_0 , and B_0' ($B_0' = \partial B / \partial P$, at $P=0$) is the first pressure derivative of the bulk modulus B . The bulk modulus B determines the compressibility and is calculated using [16]:

$$B = \left(V \frac{\partial^2 E}{\partial V^2} \right) \quad (2)$$

In fact, the bulk modulus B is quantity that defines the strength of bonds in solids; it is a measure of the solid resistance to external deformation [15].

The variation of the total energy as a function of the unit cell volume was plotted in Figs. 2 and 3 for different phases of CaMg_3 using LDA and the GGA, respectively. One can notice that CuTi_3 -type (L_{60}), AlFe_3 -type (D_{03}) and Cu_3Au -type (L_{12}) structures have almost the same minimum energy, in both LDA and GGA, while the minimum energy of αReO_3 -type (D_{09}) structure is slightly higher in both approximations. Our results of the equilibrium structural parameters,

bulk modulus and the pressure derivative of the bulk modulus of CaMg_3 in D_{03} , L_{12} , L_{60} and B_{09} structures are summarized in Table 3 together with those of the literature [8],[11].

From Table 3, we can see that the lattice constant a_0 of both AlFe_3 -type (D_{03}) and Cu_3Au -type (L_{12}) configurations are in very good agreement compared to other theoretical results [8],[11]. Our value (7.482 Å) obtained with GGA for cubic AlFe_3 -type (D_{03}) structure overestimates the theoretical value (7.48 Å) reported by Zhou and Gong, using PP-PAW (GGA) [8] by less than 0.03%, and underestimates the theoretical result (7.494 Å) reported by Groh using (MEAM) [11] by about 0.16%; while our obtained value (4.775 Å) of cubic Cu_3Au -type (L_{12}) phase underestimates the theoretical result (4.78 Å) reported by Zhou and Gong [8] by about 0.1%, and overestimates the theoretical value (4.76 Å) reported by Groh [11] by about 0.32%.

The calculated values of the bulk modulus B_0 of both D_{03} and L_{12} structures, as listed in Table 3, are slightly different from those obtained by other theoretical approaches [8],[11]; where for example, our value (33.72 GPa) obtained with GGA for D_{03} structure overestimates the theoretical value (29.57 GPa) reported by Zhou and Gong using PP-PAW (GGA) [8] by about 14%. To best of our knowledge, there are no other data existing in the literature on the structural parameters, bulk modulus and the pressure derivative of the bulk modulus for CaMg_3 compound in both L_{60} and D_{09} structures. Our findings regarding the structural parameters of CaMg_3 in both L_{60} and D_{09} structures phases perhaps can be used to predict most of the physical properties of this material. This is due to the fact that most of the physical quantities of compounds and alloys are related to the bonding of atoms, which is directly related to the structural parameters.

3.2. Structural phase transition

It is well known that high pressures influence crystal packing and electronic structure and as a result it plays an important role in materials properties, such as superconducting phenomenon, elastic properties, and structural phase transition [8]. In order to get more information about the pressure-induced phase transition of crystals, we have to calculate the Gibbs free energies G of different considered phases, which can be expressed as follows [19]–[22]:

$$G = E + PV - TS \quad (3)$$

Here E , P , V , T and S symbolize the total internal energy, pressure, volume, temperature, and entropy, respectively. Since the present calculations were performed at $T=0$ K, the term TS becomes null, and with consequence, the Gibbs free energy becomes equal to the enthalpy H [19–22]: $H = E + PV$. For CaMg_3 compound, the transition pressure (P_t) between AlFe_3 -type (D_{03}) configuration and αReO_3 -type (D_{09}) phase were calculated using the enthalpy difference as a function of the pressure with respect to D_{03} structure. Using both LDA and GGA, the variation of the enthalpy differences as a function of pressure are plotted in Fig. 4.

Table 3
Structural parameters (equilibrium lattice constants a and c/a ratio), bulk modulus B_0 and the pressure derivatives of the bulk modulus B_0' for D_{0_9} , D_{0_3} , L_{1_2} and L_{6_0} phases for $CaMg_3$ compound. a-Ref. [8] using PP-PAW (GGA), b-Ref. [11] using modified embedded-atom method (MEAM).

Phase		CaMg ₃		
Structure Type	αReO_3 -type	AlFe ₃ -type	Cu ₃ Au-type	
Symmetry	Cubic	Cubic	Cubic	
Parameter	(D _{0₉})	(D _{0₃})	(L _{1₂})	
	LDA	LDA	LDA	
a_0 (Å)	6.395 This work	7.315 7.48 ^a , 7.494 ^b Other works	4.680 4.78 ^a , 4.76 ^b Other works	4.908 GGA
B_0 (GPa)	20.077 This work	35.31 29.57 ^a , 29.87 ^b Other works	24.6 27.45 ^a , 29.29 ^b Other works	120.36 GGA
B_0'	2.876 This work	3.301 This work	3.617 This work	3.294 GGA
c/a	-	-	-	0.876 GGA
E_{min} (eV)	-34,733.2 This Work	-34,734.8 This Work	-34,737.7 This Work	-34,848.2 GGA

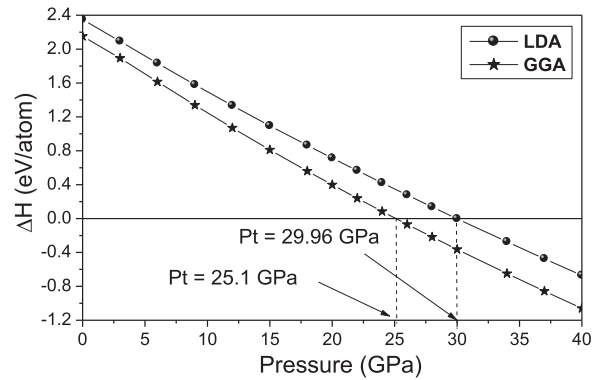


Fig. 4. Variation of the enthalpy differences ΔH as a function of pressure for $CaMg_3$ compound in αReO_3 type (D_{0_9}) phase using both LDA and GGA. The reference enthalpy in set for D_{0_3} phase.

The transition from AlFe₃-type phase (D_{0_3}) to αReO_3 -type (D_{0_9}) may occur at pressures of 29.96 GPa (from LDA calculations), and 25.1 GPa (from GGA calculations) as shown on Fig. 4. At these pressures the enthalpies of both structures become equal; and the enthalpy differences become null. Our results of the transition pressures (P_t) are in consistency with the results of Zhou and Gong [8], which found that both AlFe₃-type structure (D_{0_3}) and Cu₃Au-type structure (L_{1_2}) transform to the hexagonal close packed HCP-type structure (A3) at pressure of around 29.47 GPa and 26.44 GPa, respectively.

To best of our knowledge, there are no other data existing in the literature on the pressure-induced phase transition for $CaMg_3$ compound. Our findings regarding the pressure phase transition of $CaMg_3$ compound may be used as a reference for future works.

3.3. Electronic properties

The electronic band structures of $CaMg_3$ compound in D_{0_3} structure at the calculated equilibrium lattice constants along the high symmetry directions in the Brillouin zone are presented in Fig. 5, using both LDA and GGA. One of the most important tools to investigate the electronic structure of a metallic material is the Fermi surface; which represents the surface of constant energy in k-space [23]. The Fermi level (EF), the dashed line in Fig. 5, was set to zero energy. It is noticed that the $CaMg_3$ in D_{0_3} structure has a metallic behavior since a number of valance and conduction bands are overlapping at the Fermi level, and no band gaps exist.

Elastic constants, engineering moduli and several other related physical properties are directly related with the nature of atomic bonding in material, which can be analyzed and explained using both the total density of states (DOS) and the local density of states (LDOS) [24],[25]. The electronic density of states (EDOS) elucidates the electronic features of materials (elements, compounds, alloys, etc.) [26], the total density of states (TDOS) and partial density of states (PDOS) of $CaMg_3$ in D_{0_3} structure are calculated and presented in Fig. 6. This figure shows that the lowest lying bands are due

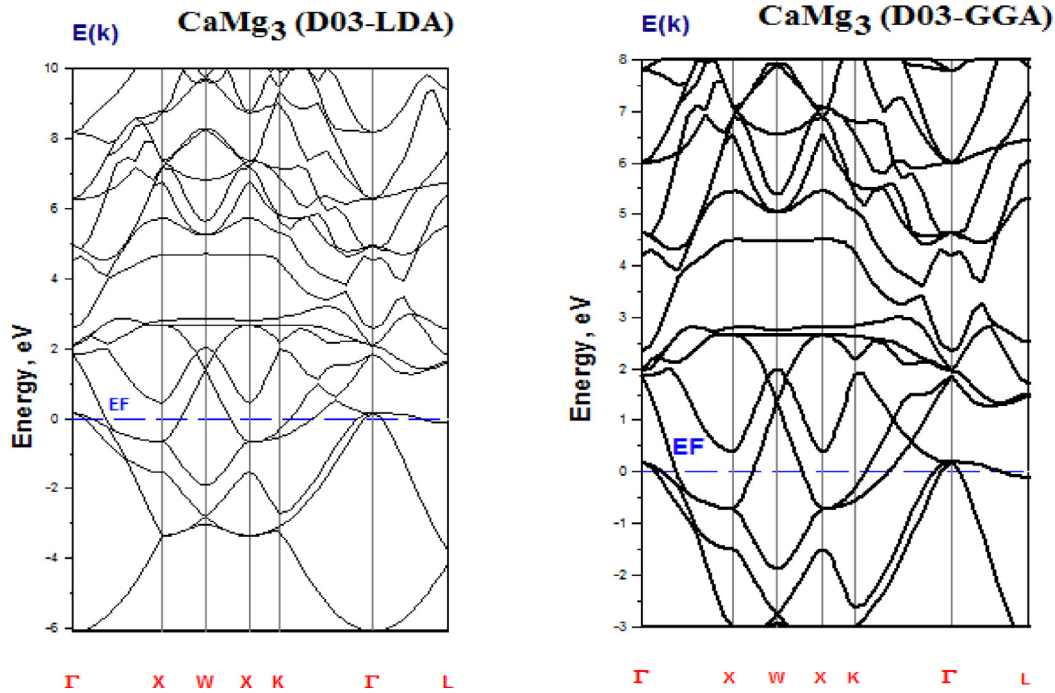


Fig. 5. Band structure of CaMg_3 compound in D0_3 structure using both LDA and GGA approaches.

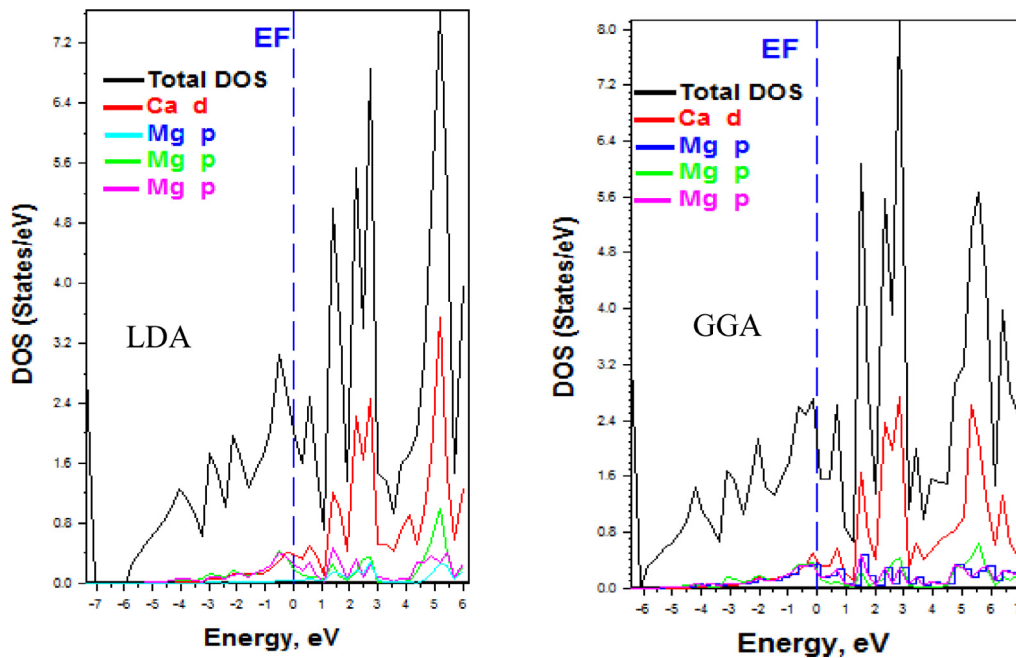


Fig. 6. Density of states (TDOS and PDOS) of CaMg_3 in D0_3 structure using both LDA and GGA.

to mainly 's' like states of Ca and do not contribute much to bonding. The valence bands in the energy range between 2 eV, and 3 eV are dominated by the maximum contribution of 'd' like states of Ca for GGA approximation, and between 4.5 and 5 eV are dominated by the maximum contribution of 'd' like states of Ca using the LDA approximation.

Moreover, the DOS at E_f of CaMg_3 in D0_3 phase were calculated, they are to be around 0.469 and 0.454 using the LDA and GGA, respectively. Our obtained values agree well with the results of Zhou and Gong [8]. The differences are around -0.061 and -0.076 using LDA and GGA, respectively.

Table 4

Calculated C_{ij} , B , G_V , G_R , G_H , E are all expressed in GPa, ν , A and G/B are without unity. Values with § are calculated using C_{ij} of Ref. [8], while those with * are calculated using C_{ij} of Ref. [11].

Parameter		C_{11}	C_{12}	C_{44}	B	G_V	G_R	G_H	E	ν	A	G/B
Our	LDA	42.34	27.25	46.65	32.28	31.01	15.18	23.09	55.94	0.21	6.18	0.72
work	GGA	37.82	25.75	48.84	29.77	31.72	12.73	22.22	53.39	0.20	8.09	0.75
Ref. [8]		37.77	25.47	47.81	29.57	31.15	12.89	22.02	52.92	0.20	7.77§	0.74
Ref. [11]		38.77	25.84	24.77	30.15*	17.45*	11.62*	14.53*	37.56*	0.29*	3.83*	0.48*

3.4. Elastic properties

3.4.1. Elastic constants, some aggregate moduli and Vickers hardness

The formation of solids is governed by the forces between the atoms, ions, and/or molecules, which are related to both the structural parameters of its crystal structure and to its chemical composition [27]. The elastic properties play an important role in the structural stability and stiffness of materials. In cubic structures, as in the case of $D0_3$ structure of CaMg_3 compound, there are three independent elastic stiffness constants, namely: C_{11} , C_{12} and C_{44} , that were obtained in the present work by calculating the total energy as a function of strain [16],[28]. The determination of the elastic constants C_{ij} needs the knowledge of the nature of the strain, which is expressed as follow [16]:

$$\bar{\epsilon} = \begin{bmatrix} \delta & 0 & 0 \\ 0 & -\delta & 0 \\ 0 & 0 & \frac{\delta^2}{(1-\delta^2)} \end{bmatrix} \quad (4)$$

Applying this tensor strain modifies the total energy from its unstrained value to the following expression [16]:

$$E(\delta) = E(0) + 3(C_{11} - C_{12})V_0\delta^2 + 0(\delta^4) \quad (5)$$

where $E(0)$ is the energy of the unstrained lattice of unit cell volume V_0 .

The identification of C_{44} is through the volume-conserving tetragonal strain tensor [16]:

$$\bar{\epsilon} = \begin{bmatrix} \frac{\delta}{2} & 0 & 0 \\ 0 & -\frac{\delta}{2} & 0 \\ 0 & 0 & \frac{\delta^2}{(4-\delta^2)} \end{bmatrix} \quad (6)$$

The total energy is given as follow [16]

$$E(\delta) = E(-\delta) = E(0) + \frac{1}{2}C_{44}V_0\delta^2 + 0(\delta^4) \quad (7)$$

Our results of the elastic constants (C_{11} , C_{12} and C_{44}) obtained from both LDA and GGA approximations are presented in Table 4. Except of two theoretical works based on DFT and MEAM, by Zhou and Gong [8] and Groh [11], respectively, there are no other theoretical or experimental values available, to the best of our knowledge, for the elastic constants of CaMg_3 in $D0_3$ phase. Using the calculated values of the elastic constants, other elastic parameters can be calculated such as: bulk modulus B , Voigt, Reuss and Hill shear moduli (G_V , G_R , G_H), Young's modulus E , Poisson's ratio ν , anisotropy factor A and Pugh's ratio (G/B) using the following equations [16],[28],[29]:

$$B = \frac{C_{11} + 2C_{12}}{3} \quad (8)$$

$$G_V = \frac{C_{11} - C_{12} + 3C_{44}}{5}, \quad (9)$$

$$G_R = \frac{5C_{44}(C_{11} - C_{12})}{4C_{44} + 3(C_{11} - C_{12})} \quad (10)$$

$$G_H = \frac{1}{2}(G_V + G_R) \quad (11)$$

$$E = \frac{9BG}{G + 3B} \quad (12)$$

$$\nu = \frac{3B - 2G}{2(3B + G)} \quad (13)$$

$$A = \frac{2C_{44}}{C_{11} - C_{12}} \quad (14)$$

Our results of the elastic stiffness constants C_{ij} and the other elastic parameters above obtained for $D0_3$ phase of CaMg_3 phase using both LDA and GGA approximations are presented in Table 4. Except of two theoretical works based on DFT and MEAM, realized by Zhou and Gong [8] and Groh [11], respectively, to the best of our knowledge, there are no other theoretical or experimental values available for the elastic constants of CaMg_3 in $D0_3$ phase.

A look on Table 4, shows that the calculated elastic constants C_{ij} satisfied elastic stability criteria: $(C_{11} - C_{12}) > 0$, $C_{11} > 0$, $C_{44} > 0$, $(C_{11} + 2C_{12}) > 0$, $C_{12} < B < C_{11}$ [30],[31]. At normal conditions, the mechanical stability of CaMg_3 in $D0_3$ phase was also found in previous calculations reported by Zhou and Gong [8] and Groh [11]. One can also notice, from Table 4, that the elastic constant C_{11} (related to the axial compression along the principal crystallographic directions [32]) is slightly lower than C_{44} , indicating that CaMg_3 compound in $D0_3$ phase presents a higher resistance to pure shear deformation compared to the axial compression resistance. The same behavior was also noticed by Zhou and Gong [8] using the same approach (DFT) like ours, but not observed in the work of Groh [11], which used a different formalism (the second nearest-neighbors modified embedded-atom method (MEAM)).

Another note, from Table 4, that our values of the elastic stiffness constant C_{ij} and other elastic moduli of CaMg_3 compound in $D0_3$ structure are in excellent agreement with the results of Zhou and Gong [8] and Groh [11], except for C_{44} , where for example, our value (29.77 GPa) of the bulk

modulus B obtained with GGA overestimates the theoretical value (29.57 Å) reported by Zhou and Gong [8] by around 0.68%.

The Poisson's ratio ν is small (usually $\nu < 0.1$) for covalent materials, while for ionic materials, ν is 0.25 [33],[34]. Therefore, in CaMg_3 compound in D0_3 structure (where $\nu \sim 0.20$), a higher ionic contribution in an intra-atomic bonding is expected.

Young's modulus E is an important indicator on elasticity; materials having higher values of E , are more stiffer. Our obtained value of E for CaMg_3 compound in D0_3 phase was found at around 55.94 GPa using LDA, and 53.39 GPa using GGA, respectively. These two values are slightly higher than the Young modulus (41.43 GPa) reported by Daoud et al. [35] for MgCa in B2 phase.

On the other hand, the shear modulus G , which can be obtained from the measure of resistance to the reversible deformation under the applied shearing stress, plays a dominant role in predicting the hardness of the material [36]. The Pugh's ratio G/B has been extensively used as an empirical parameter to express the brittleness/ductility of materials [8]. The critical value of G/B ratio that separates the brittle/ductile behavior is 0.57 ($B/G = 1.75$); a larger G/B value means more brittleness, and vice versa [8]. It can be seen from Table 4 that our values of G/B ratio obtained using both LDA and GGA for CaMg_3 compound in D0_3 structure are in good agreement with the results of Zhou and Gong [8]. The values of G/B ratio are greater than 0.57, indicating the brittleness nature of CaMg_3 compound in D0_3 phase. This conclusion was also confirmed from the values of the Poisson's ratio ($\nu \sim 0.20$) which is smaller than the critical value $\nu = 0.26$ [16]. It should be noted that, if we use the elastic stiffness constant C_{ij} obtained by Groh [11], a value of ~ 0.48 for the G/B ratio will be found.

Liu et al. [37] reported that the ductility is a shear-related mechanical property of material, it is associated with both the elastic constant C_{44} and the density of states (DOS) at Fermi energy, while Daoud et al. [35] showed an anti-correlation between the elastic constant C_{44} and the DOS at Fermi energy in MgCa intermetallic compound under compression. This anti-correlation perhaps explained by the fact that as the total DOS at Fermi level increases covalent/ionic behavior, gradually transformed into metallic behavior, thus turning the brittle phase into a ductile one [35].

The Vickers hardness H_V measurement is one of the most techniques used in the mechanical characterization of the materials [35]. Like refractive index and density, hardness is a intrinsic property of the given crystal [36]. The Vickers hardness H_V , the bulk modulus B and the shear modulus G are related by the empirical formula [35]:

$$H_V = 0.92(G/B)^{1.137} \times G^{0.708} \quad (15)$$

Using our values of the bulk modulus B and the shear modulus G obtained from the LDA and GGA, the present results of the Vickers hardness H_V for CaMg_3 compound in D0_3 phase are: 5.80 and 5.93 GPa, respectively. These two values are slightly higher than the Vickers hardness H_V (4.82 GPa)

of MgCa intermetallic compound in B2 phase [35]. As far as we know, there are no data available related to Vickers hardness H_V in the literature for CaMg_3 in D0_3 phase, therefore our calculated values can be considered as prediction for this property for this material.

3.4.2. Elastic wave speeds and Debye temperature

The Debye temperature θ_D parameter is related to many important physical properties of solids, such as specific heat and melting temperature [32]. It is either measured from the elastic constants, or from the specific heat measurement [38]. However, at low temperatures both methods give almost the same value of θ_D , since at low temperature the vibrational excitations arise from acoustic modes only. The Debye temperature θ_D may be estimated from the average sound velocity v_m by the following equation [16]:

$$\theta_D = \frac{h}{k_B} \left(\frac{3}{4\pi V_a} \right)^{\frac{1}{3}} v_m \quad (16)$$

where h is Planck's constant, k_B Boltzmann's constant, and V_a is the atomic volume.

Usually, the average sound velocity v_m of the aggregate material can be calculated from the longitudinal (compressed) v_l and transverse (shear) v_t sound velocities as follows [39],[40]

$$v_m = \left[\frac{1}{3} \left(\frac{2}{v_t^3} + \frac{1}{v_l^3} \right) \right]^{-\frac{1}{3}} \quad (17)$$

The crystal density ρ is usually expressed in g/cm^3 (or in kg/m^3); it is given as follow [41–43]

$$\rho = MZ/N_A V \quad (18)$$

where M is the molecular weight, usually expressed in 10^{-3}kg , Z is the number of molecules per unit cell, $N_A (= 6.022 \times 10^{23} \text{ mol}^{-1})$ is the Avogadro's number, while V is the unit cell volume usually expressed in m^3 . For CaMg_3 compound in D0_3 phase, the number of molecules per unit cell Z was taken equal to four, and the unit cell volume V was taken equal to a^3 , while a is lattice constant. Adachi [44] has mentioned that the lattice parameters are related to the pressure by Murnaghan equation of state, and they are influenced by the crystalline perfection, such as: impurities, stoichiometry, dislocations and surface damage. Table 5 summarize the results of the crystal density ρ , the average elastic wave velocity v_m , the longitudinal wave velocity v_l and the transverse acoustic wave velocity v_t as well as the Debye temperature θ_D of CaMg_3 compound in D0_3 phase, which could not be compared due to unavailability of the measured data.

A look on Table 5, the Debye temperature θ_D of CaMg_3 in D0_3 phase was found at around 393.44 K using LDA, and 389.91 K using GGA, respectively. Since the Debye temperature θ_D correlates with the Young's modulus E in cubic perovskite-type RBRh_3 (R are Sc, Y, La and Lu) materials [45], these two values of θ_D are also slightly higher than the Debye temperature θ_D (328.65 K) reported by Daoud et al. [35] for MgCa in B2 phase. Although this rationalization may

Table 5

Crystal density ρ , sound velocities v_l , v_t , v_m Debye temperature θ_D and the limiting angular vibrational frequency ω_D for CaMg₃ compound in D0₃ phase. Values with § are calculated using the data of Ref. [8], while those with * are calculated using the data of Ref. [11].

Parameter	ρ (kg/m ³)	v_l (m/s)	v_t (m/s)	v_m (m/s)	θ_D (K)	ω_D (10 ¹³ rad/s)
This work (LDA)	1917.42	3470.48	5735.34	3835.99	393.44	5.93
This work (GGA)	1791.88	3521.67	5757.77	3888.34	389.91	5.88
Ref. [8]	1793.31 [§]	3503.9 [§]	5732.26 [§]	3868.97 [§]	388.07 [§]	5.85 [§]
Ref. [11]	1783.28*	2854.61*	5269.92*	3185.47*	318.91*	4.81*

be useful for chemically related compounds, compounds that are significantly different in chemical nature perhaps should not be necessary expected to follow the same correlation.

We have also calculated the Debye temperature θ_D for CaMg₃ in D0₃ phase using a semi-empirical formula between θ_D and elastic constants C_{ij} first proposed by Blackmann [46], and latter used by Siethoff and Ahlborn [47] after improvements for several crystals with different structures. This semiempirical formula can be written as [48]

$$\theta_D = C_B(aG_B/M)^{1/2},$$

$$G_B = [C_{44}(C_{11} - C_{12})(C_{11} - C_{12} + 2C_{44})]^{1/3}, \quad (19)$$

where a is the lattice constant, M is the atomic weight (for compounds, M is the weighted arithmetical average of the masses of the species), and $C_B = 3.89 \times 10^{11} \times n^{-1/6} h/k_B$ is a model parameter. In this model parameter, h ($= 6.62617 \times 10^{-34}$ J.s), k_B ($= 1.38062 \times 10^{-23}$ J.K⁻¹) and n are Planck's constant, Boltzmann's constant and the number of atoms in the unit cell, respectively. More details can be found in Refs. [48].

Using Eq. (19), the Debye temperature θ_D of CaMg₃ in D0₃ phase was found at around 417.16 K using LDA, and 408.91 K using GGA, respectively. These two values of θ_D are slightly higher than the values 393.44 K (LDA) and 389.91 K (GGA) obtained from Eq. (16).

From Debye temperature one can estimate the Debye cut-off frequency (the limiting angular vibrational frequency) ω_D by the following expression [49]:

$$\omega_D = k_B\theta_D/\hbar \quad (20)$$

where k_B is Boltzmann's constant, and $\hbar = h/2\pi$, h is Planck's constant.

Substituting the values (393.44 K, and 389.91 K) of the Debye temperature θ_D , obtained from the LDA and GGA, in Eq. (20), the present results of the limiting angular vibrational frequency ω_D for CaMg₃ compound in D0₃ phase are: 5.93×10^{13} and 5.88×10^{13} rad/s, respectively. These results as well as those calculated from the data of Refs. [8],[11] are also summarized in Table 5.

The same as in the case of the elastic constants and the structural parameters, the longitudinal, transverse and average sound velocities as well as the Debye temperature of our material of interest are in excellent agreement with those calculated using the data of Ref. [8] obtained from the same approach (DFT). To the best of our knowledge, there are no other theoretical or experimental data existing in the literature on the sound velocity, Debye temperature, and Debye cut-off

frequency for CaMg₃ in D0₃ structure. So, we think that our findings regarding these quantities can be used to predict and explain most of the physical properties of this material.

4. Conclusion

In this work, we have investigated the equilibrium structural parameters of CaMg₃ compound in α ReO₃-type (D0₉), AlFe₃-type (D0₃), Cu₃Au -type (L1₂) and CuTi₃-type (L6₀) configurations using an *ab-initio* FP-LMTO method, within both local density approximation (LDA), and generalized gradient approximation (GGA). At equilibrium our results for the EOS parameters, in general, agreed well with other data of the literature.

The results of the present work concerned with the possibility of phase transition at high pressure show that CaMg₃ transforms from AlFe₃-type structure (D0₃) to α ReO₃-type (D0₉) at pressure of around 29.96 GPa using LDA, and at around 25.1 GPa using the GGA.

Both LDA and GGA approaches for the electronic band structures, the total density of states (TDOS) as well as the partial density of states (PDOS) showed that CaMg₃ in D0₃ phase has a metallic behavior.

The elastic constants, Young's modulus, shear modulus, Poisson's ratio, index of ductility, Vickers hardness, sound velocities, Debye temperature, and the limiting angular vibrational frequency of CaMg₃ in D0₃ phase were also reported. Our findings on the elastic constants were also in agreed well with other theoretical data of the literature.

References

- [1] J. Zhang, S. Liu, R. Wu, L. Hou, M. Zhang, J. Magnes. Alloys 6 (2018) 277, doi:10.1016/j.jma.2018.08.001.
- [2] R.H. Taylor, S. Curtarolo, G.L.W. Hart, Phys. Rev. B 84 (2011) 084101, doi:10.1103/physrevb.84.084101.
- [3] S. Daoud, N. Bioud, P.K. Saini, J. Magnes. Alloy. 7 (2019) 335, doi:10.1016/j.jma.2019.01.006.
- [4] S. Boucetta, F. Zegrar, J. Magnes. Alloy. 1 (2013) 128, doi:10.1016/j.jma.2013.05.001.
- [5] H. Si, Y. Jiang, Y. Tang, L. Zhang, J. Magnes. Alloy. 7 (2019) 501, doi:10.1016/j.jma.2019.04.006.
- [6] N. Sezer, Z. Evis, S.M. Kayhan, A. Tahmasebifar, M. Koç, J. Magnes. Alloy. 6 (2018) 23.
- [7] A.-I. Bitu, I. Antoniac, I. Ciuca, U. P. B. Sci. Bull., Series B 78 (2016) 173.
- [8] P. Zhou, H.R. Gong, J. Mech. Behav. Biomed. Mater. 8 (2012) 154, doi:10.1016/j.jmbbm.2011.12.001.
- [9] N. Bioud, K. Kassali, X.-W. Sun, T. Song, R. Khenata, S. Bin-Omran, Mater. Chem. Phys. 203 (2018) 362, doi:10.1016/j.matchemphys.2017.10.016.

- [10] R. Yagoub, H. Rekab-Djabri, S. Daoud, S. Louhibi-Fasla, M.M.A. Salam, S. Bahlouli, M. Ghezali, *Comput. Condens. Matter.* 23 (2020) e00452, doi:10.1016/j.cocom.2019.e00452.
- [11] S. Groh, *J. Mech. Behav. Biomed. Mater.* 42 (2015) 88, doi:10.1016/j.jmbbm.2014.11.012.
- [12] J.P. Perdew, Y. Wang, *Phys. Rev. B* 45 (1992) 13244, doi:10.1103/PhysRevB.45.13244.
- [13] J.P. Perdew, S. Burke, M. Ernzerhof, *Phys. Rev. Lett.* 77 (1996) 3865, doi:10.1103/PhysRevLett.77.3865.
- [14] S.Y. Savrasov, *Phys. Rev. B* 54 (1996) 16470.
- [15] A. Rastogi, P. Rajpoot, U.P. Verma, *Bull. Mater. Sci.* 42 (2019) 112, doi:10.1007/s12034-019-1758-8.
- [16] H. Rekab-Djabri, M. Drief, M.M. Abdus Salam, S. Daoud, F. El Haj Hassan, S. Louhibi-Fasla, *Can. J. Phys.* (2020), doi:10.1139/cjp-2019-0357.
- [17] G. Murtaza, A.A. Khan, M. Yaseen, A. Laref, N. Ullah, I.U. Rahman, *Chinese Phys. B* 27 (2018) 047102.
- [18] S. Daoud, N. Bioud, N. Lebga, *Chinese J. Phys.* 57 (2019) 165, doi:10.1016/j.cjph.2018.11.018.
- [19] S. Zerroug, F. Ali Sahraoui, N. Bouarissa, *Appl. Phys. A* 97 (2009) 345.
- [20] H. Rekab-Djabri, R. Khatir, S. Louhibi-Fasla, I. Messaoudi, H. Achour, *Comput. Condens. Matter.* 10 (2017) 15.
- [21] S. Daoud, N. Bouarissa, *Comput. Condens. Matter.* 19 (2019) e00359, doi:10.1016/j.cocom.2018.e00359.
- [22] Y.O. Ciftci, E. Ateser, *J. Electron. Mater.* 49 (2020) 2086, doi:10.1007/s11664-019-07891-3.
- [23] E. Viswanathan, M. Sundareswari, D.S. Jayalakshmi, M. Manjula, *Comput. Mater. Sci.* 157 (2019) 107.
- [24] X. Zhou, D. Gall, S.V. Khare, *J. Alloys Compd.* 595 (2014) 80.
- [25] J.A. Warner, S.K.R. Patil, S.V. Khare, K.C. Masiulaniec, *Appl. Phys. Lett.* 88 (2006) 101911.
- [26] M.N. Rasul, A. Anam, M.A. Sattar, A. Manzoor, A. Hussain, *Chinese J. Phys.* 59 (2018) 656.
- [27] S. Daoud, N. Bouarissa, N. Bioud, P.K. Saini, *Chem. Phys.* 56 (2018) 2659–2672, doi:10.1016/j.chemphys.2019.110399.
- [28] M.J. Mehl, J.E. Osburn, D.A. Papaconstantopoulos, B.M. Klein, *Phys. Rev. B* 41 (1990) 103112.
- [29] R. Hill, *Proc. Phys. Soc. Lond. A* 65 (1952) 349.
- [30] G.V. Sin'ko, N.A. Smirnov, *J. Phys. Condens. Matter.* 14 (2002) 6989.
- [31] A. Benmakhlouf, A. Benmakhlouf, O. Allaoui, S. Daoud, *Chinese J. Phys.* 59 (2019) 656, doi:10.1016/j.cjph.2019.04.010.
- [32] A. Benmakhlouf, A. Benmakhlouf, O. Allaoui, S. Daoud, *Chinese J. Phys.* 57 (2019) 179, doi:10.1016/j.cjph.2018.11.017.
- [33] J. Haines, J.M. Leger, G. Bocquillon, *Annu. Rev. Mater. Res.* 31 (2001) 1.
- [34] T. Usman, G. Murtaza, H. Luo, A. Mahmood, *J. Supercond. Nov. Magn* 30 (2017) 1389.
- [35] S. Daoud, N. Bouarissa, A. Benmakhlouf, O. Allaoui, *Phys. Status Solidi B* 257 (2020) 1900537, doi:10.1002/pssb.201900537.
- [36] M.Sundareswari E.Viswanathan, *J. Chem. Pharm. Sci.* 11 (2015) 11.
- [37] Z.T.Y. Liu, D. Gall, S.V. Khare, *Phys. Rev. B* 90 (2014) 134102.
- [38] N. Bioud, X.-W. Sun, N. Bouarissa, S. Daoud, *Z. Naturforsch. A* 73 (2018) 767, doi:10.1515/zna-2018-0120.
- [39] S. Daoud, *Comput. Mater. Sci.* 111 (2016) 532, doi:10.1016/j.commatsci.2015.09.022.
- [40] P.K. Saini, D.S. Ahlawat, S. Daoud, D. Singh, *Ind. J. Pure. Appl. Phys.* 57 (2019) 793 <http://noprniscair.res.in/handle/123456789/51725>.
- [41] R.E. Newnham, in: *Properties of Materials: Anisotropy, Symmetry, Structure*, Oxford University Press, 2005, p. 5.
- [42] S. Daoud, *Eur. Phys. J. B* 89 (2016) 47, doi:10.1140/epjb/e2016-60844-9.
- [43] S. Daoud, *Mater. Res.* 19 (2016) 314, doi:10.1590/1980-5373-MR-2015-0602.
- [44] S. Adachi, *Properties of Group-IV, III-V and II-VI Semiconductors*, John Wiley & Sons Ltd, 2005.
- [45] A. Bouhemadou, G. Uğur, S. Uğur, F. Soyalp, R. Khenata, S. Bin-Omran, *Comput. Mater. Sci.* 54 (2012) 336, doi:10.1016/j.commatsci.2011.10.029.
- [46] M. Blackmann, *Philos. Mag.* 42 (1951) 1441, doi:10.1080/14786445108560963.
- [47] H. Siethoff, K. Ahlborn, *Phys. Status Solidi B* 190 (1995) 179.
- [48] P.K. Jha, M. Talati, *Phys. Status Solidi B* 239 (2003) 291, doi:10.1002/pssb.200301829.
- [49] M. Kaviani, *Heat Transfer Physics*, Cambridge University Press, 2008.